Detecting ultralight dark matter with trapped-ion interferometers

Leonardo Badurina
with Diego Blas, Sebastian A. R. Ellis, and John R. Ellis

Based on 2507.XXXX

PASCOS 2025

The dark matter landscape

The dark matter landscape

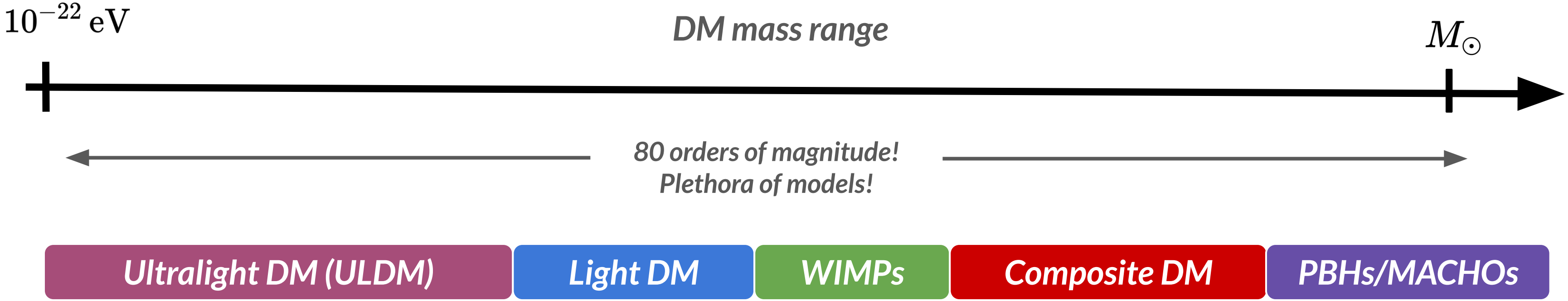

The dark matter landscape

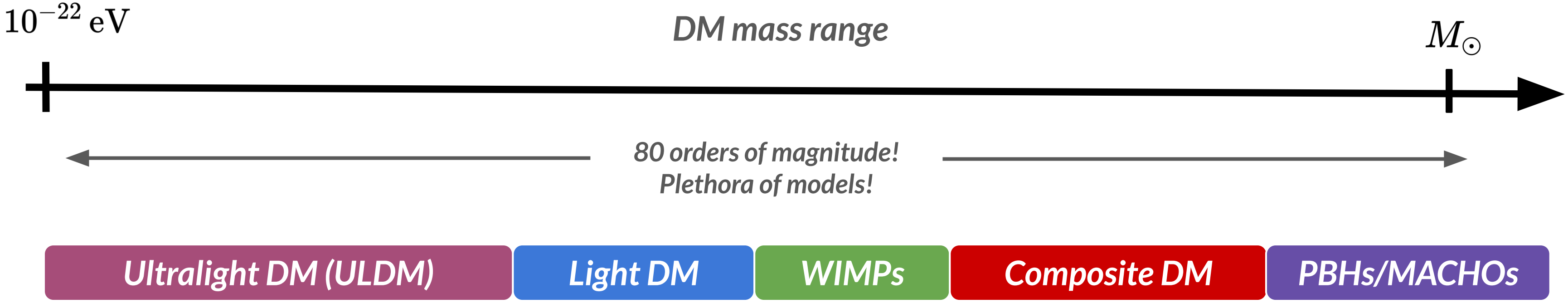

Many different interactions & many different probes

The dark matter landscape

Many different interactions & many different probes

Examples: coupling to photons, axion-like particles (ALPs)

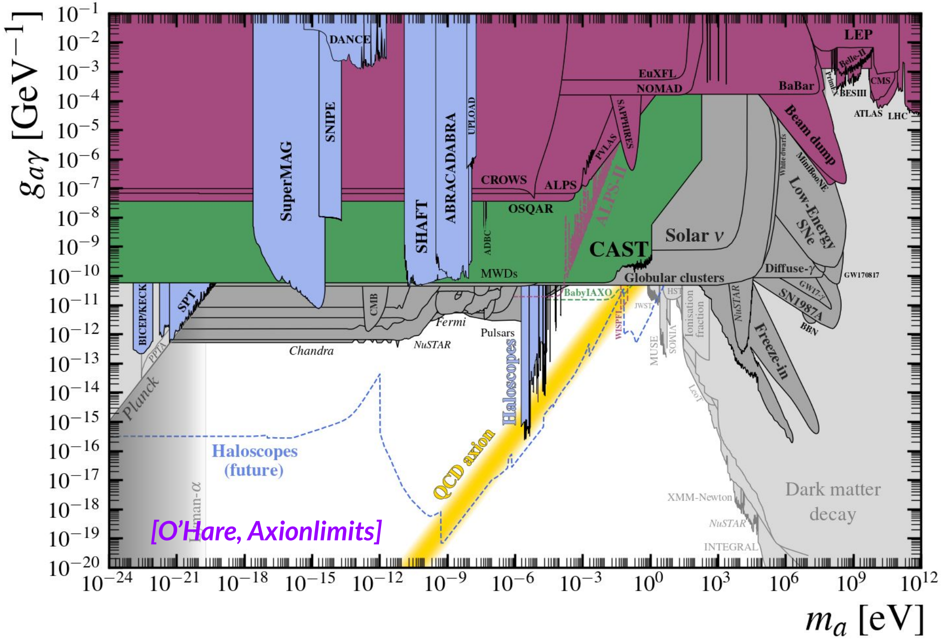

The dark matter landscape

Many different interactions & many different probes

Examples: coupling to photons, kinetically-mixed dark photons

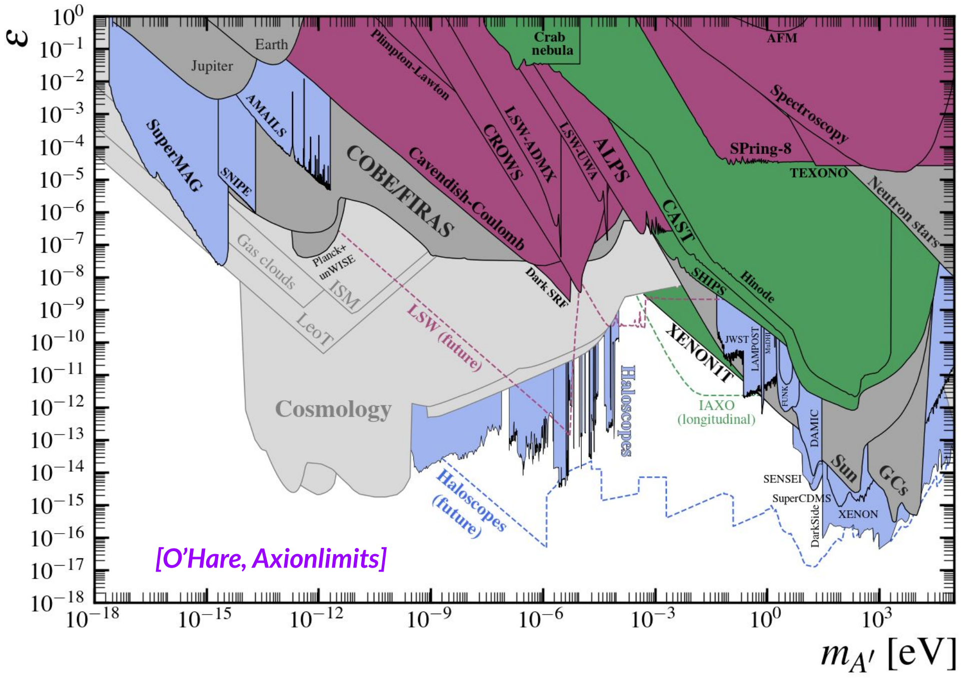

[O'Hare, Axionlimits]

Motivation

Can we leverage quantum sensing techniques to probe unexplored regions of DM model space with tabletop experiments?

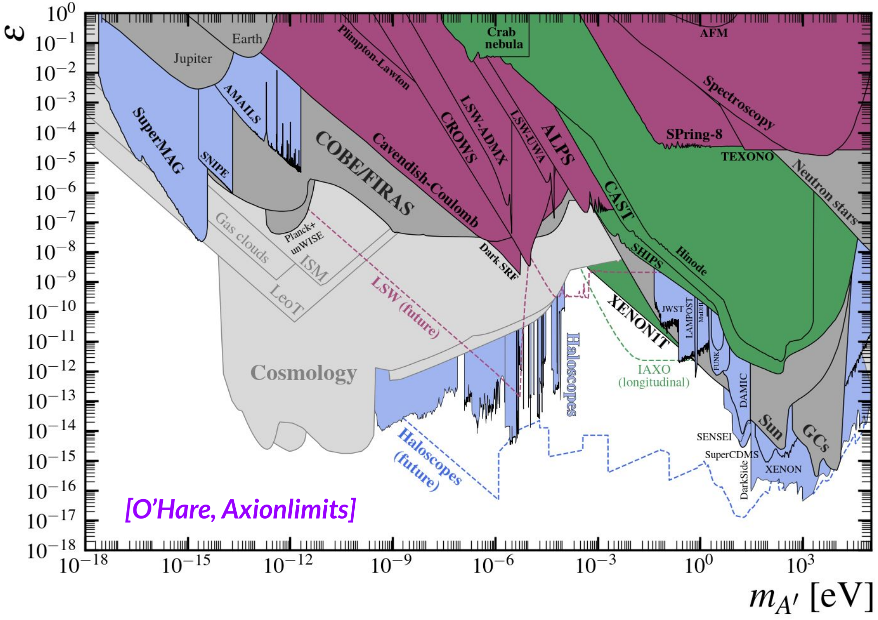

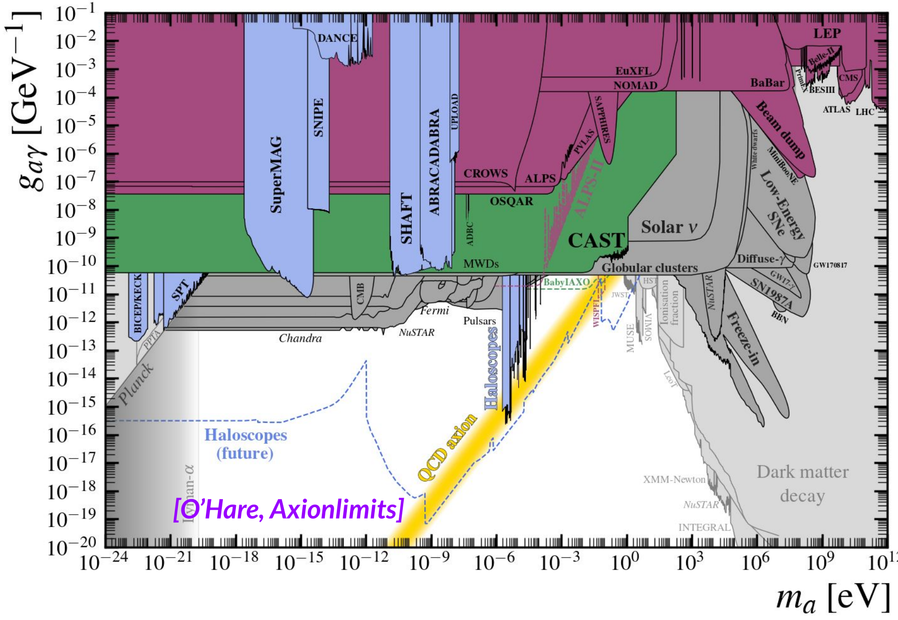

Motivation

Can we leverage quantum sensing techniques to probe unexplored regions of DM model space with tabletop experiments?

Yes, by measuring DM-sourced magnetic fields with trapped-ion interferometry

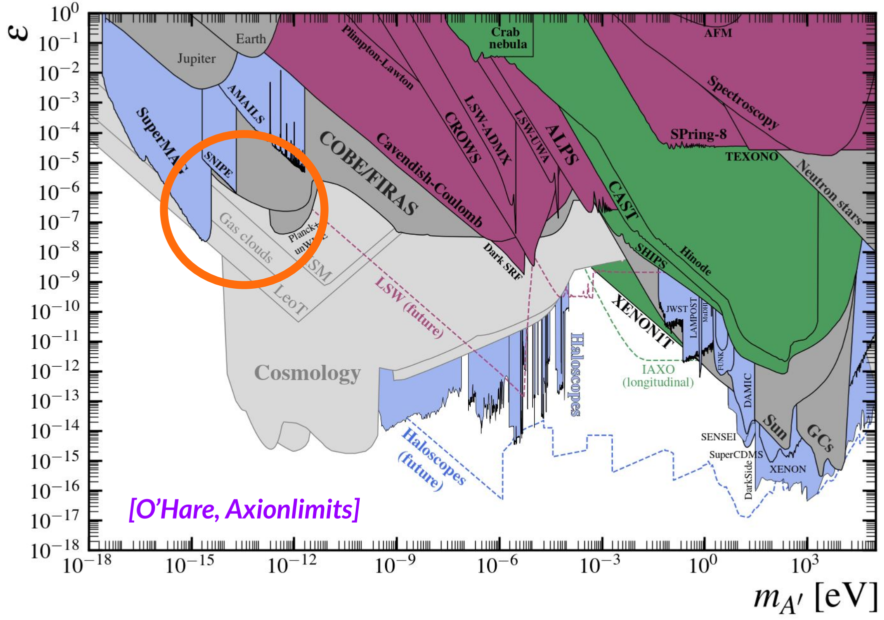

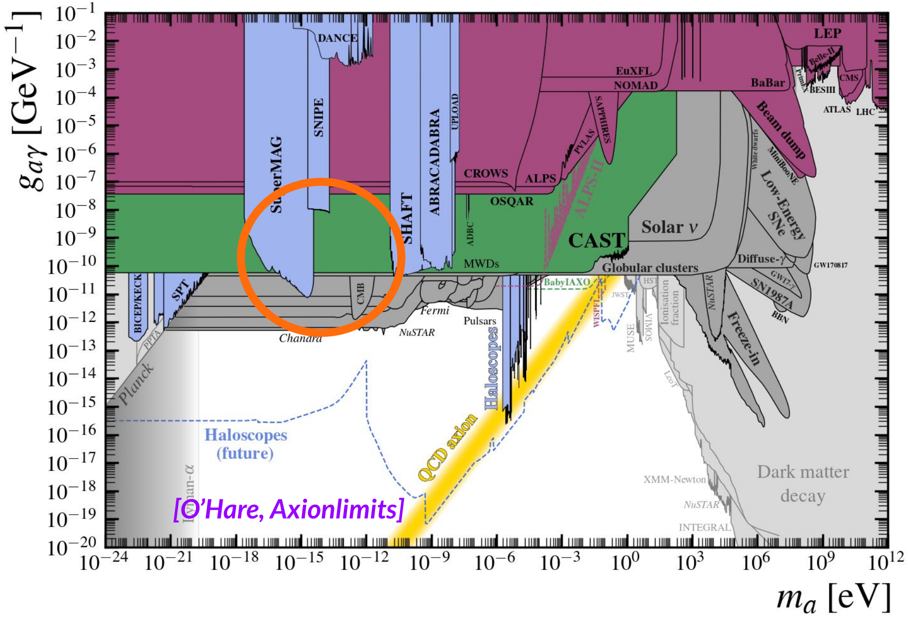

Key features of trapped-ion interferometry

Proposal developed by Wes Campbell and Paul Hamilton for rotation sensing [JPB, 2017]

Key features of trapped-ion interferometry

Proposal developed by Wes Campbell and Paul Hamilton for rotation sensing [JPB, 2017]

Key features:

Key features of trapped-ion interferometry

Proposal developed by Wes Campbell and Paul Hamilton for rotation sensing [JPB, 2017]

Key features:

Matter-wave interferometry (Ramsey sequence) with electrically charged states

Key features of trapped-ion interferometry

Proposal developed by Wes Campbell and Paul Hamilton for rotation sensing [JPB, 2017]

Key features:

Matter-wave interferometry (Ramsey sequence) with electrically charged states

Entanglement of spin and motional degrees of freedom

Magnetically-insensitive states -> long coherence times of the excited state

Key features of trapped-ion interferometry

Proposal developed by Wes Campbell and Paul Hamilton for rotation sensing [JPB, 2017]

Key features:

Matter-wave interferometry (Ramsey sequence) with electrically charged states

Entanglement of spin and motional degrees of freedom

Magnetically-insensitive states -> long coherence times of the excited state

Harmonic and rotationally symmetric potential in 2D

Excellent control over systematics [West, PRA 2019]

A sketch of trapped-ion interferometry

Step 1: ion is prepared in the spin down state and placed at the centre of the trap

position space

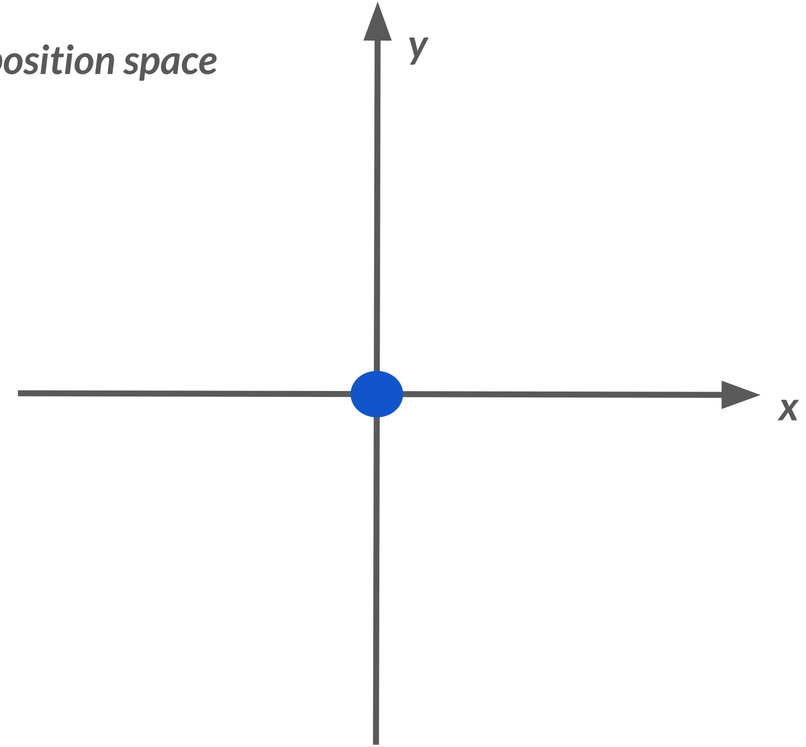

x-phase space

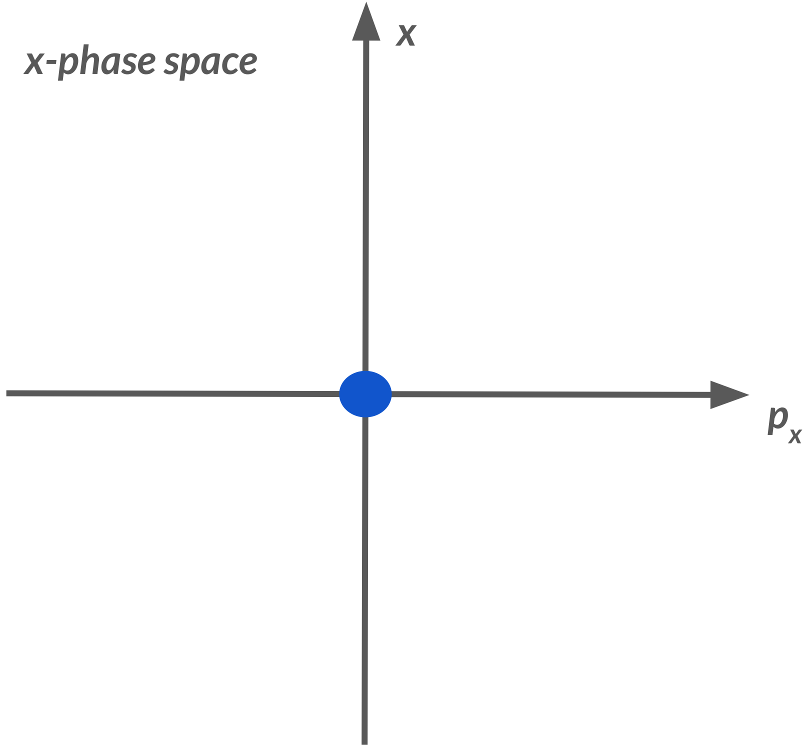

A sketch of trapped-ion interferometry

Step 2: apply a beam-splitter pulse

position space

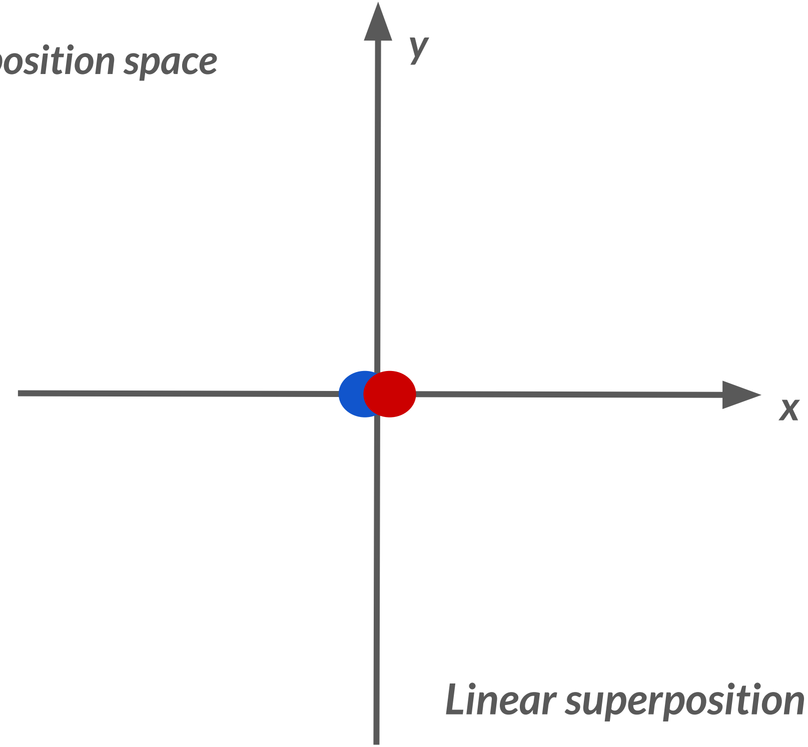

x-phase space

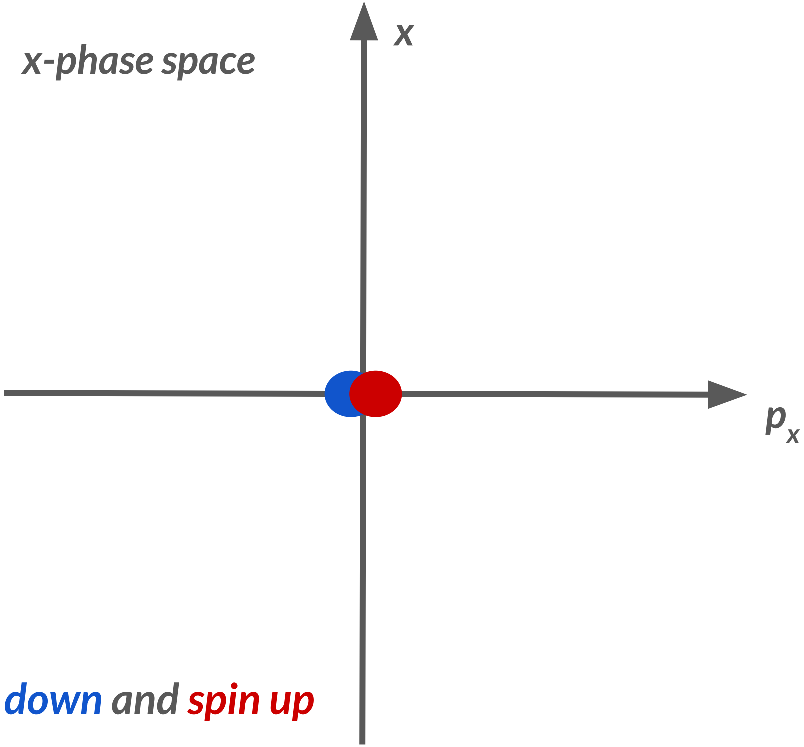

Linear superposition of spin down and spin up

A sketch of trapped-ion interferometry

Step 3: apply N successive spin-dependent laser kicks (SDKs) in the x-direction

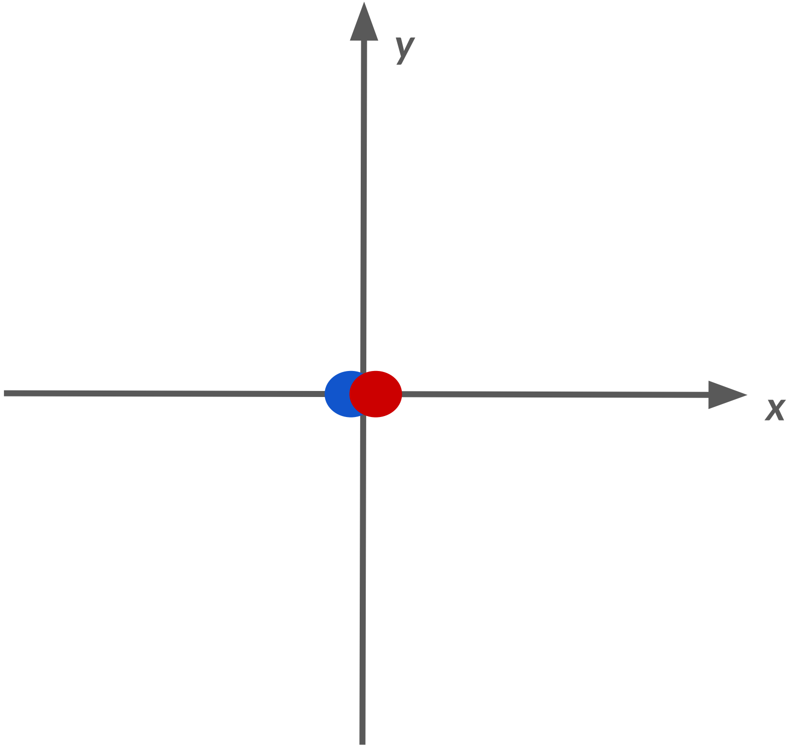

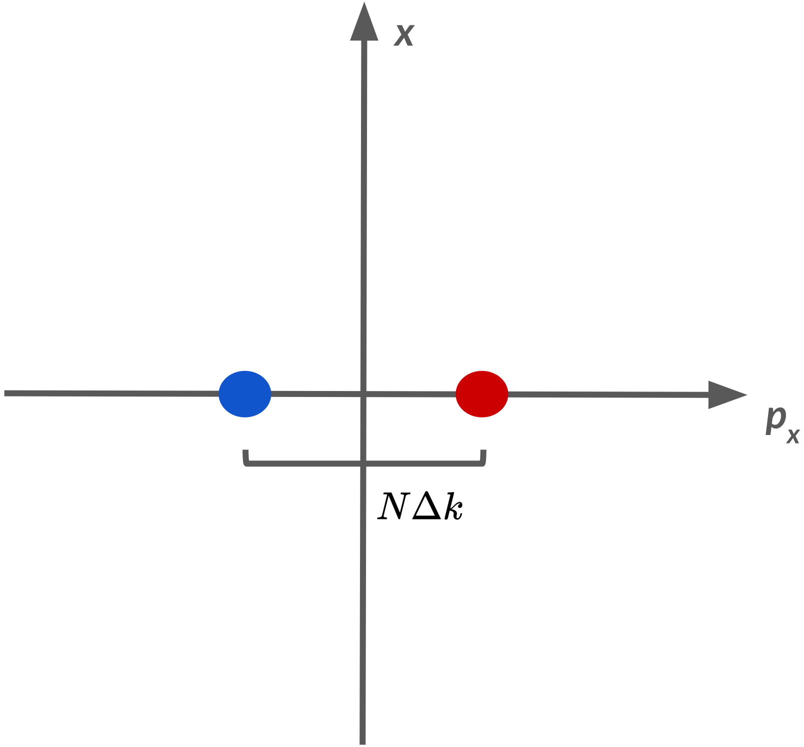

A sketch of trapped-ion interferometry

Step 4: non-adiabatic displacement of the trap centre in the y-direction

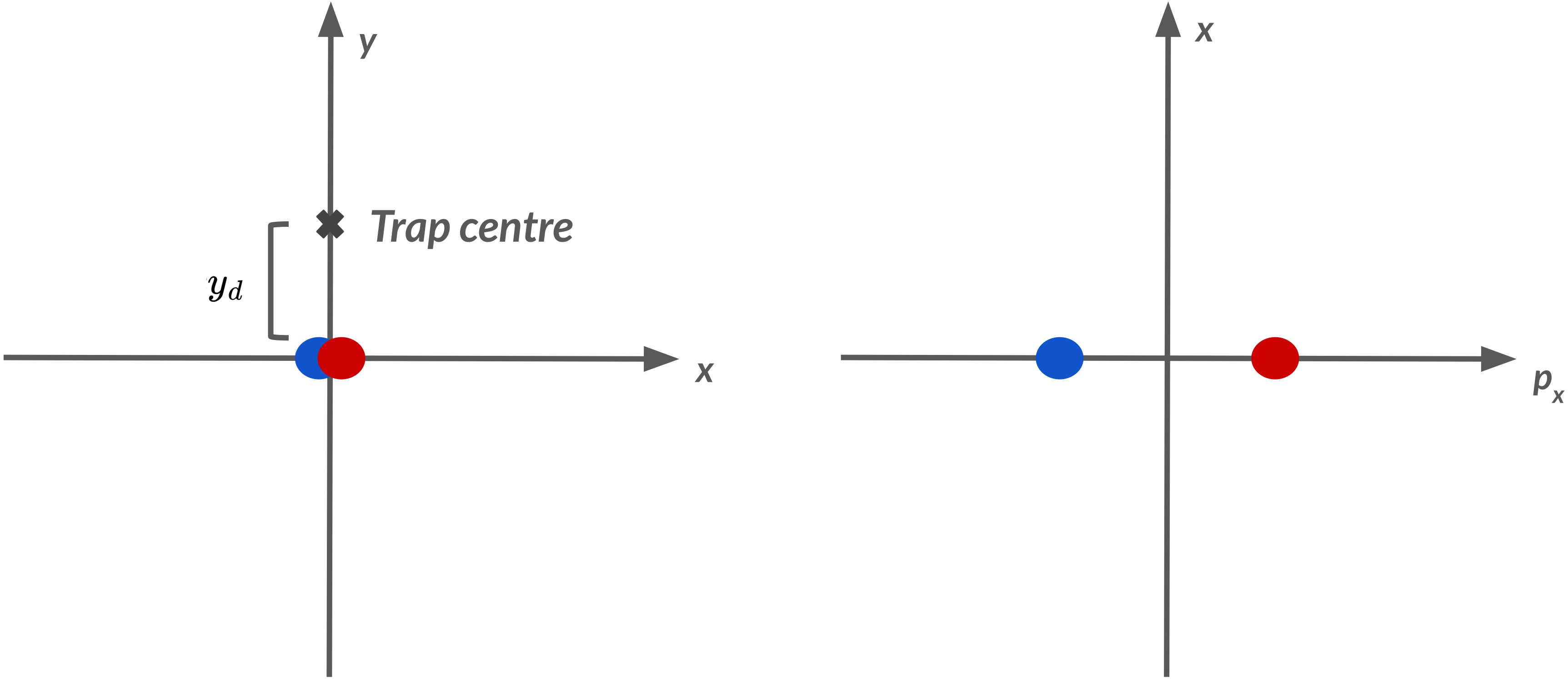

A sketch of trapped-ion interferometry

Step 5: free evolution of the ions in the trap

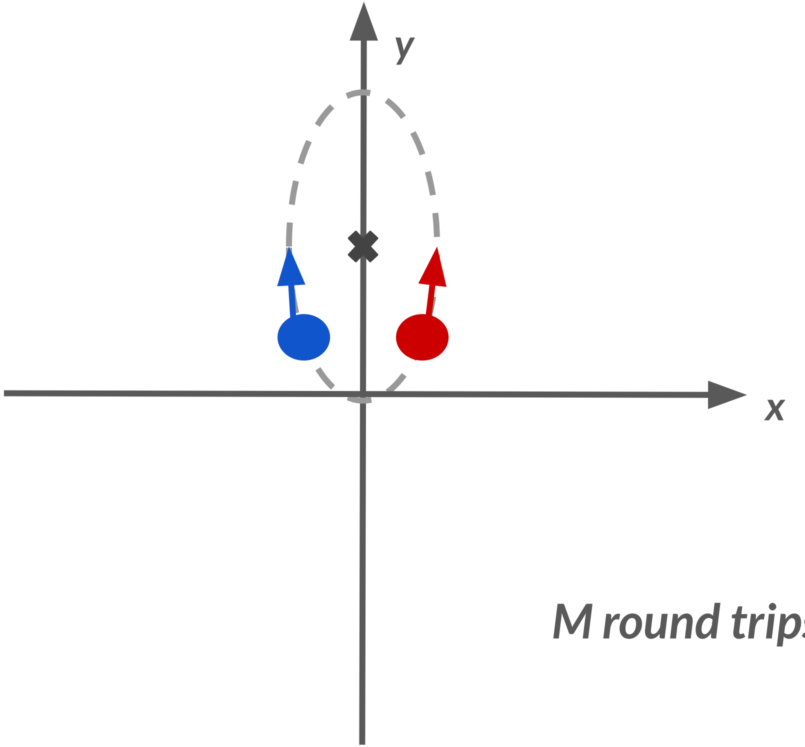

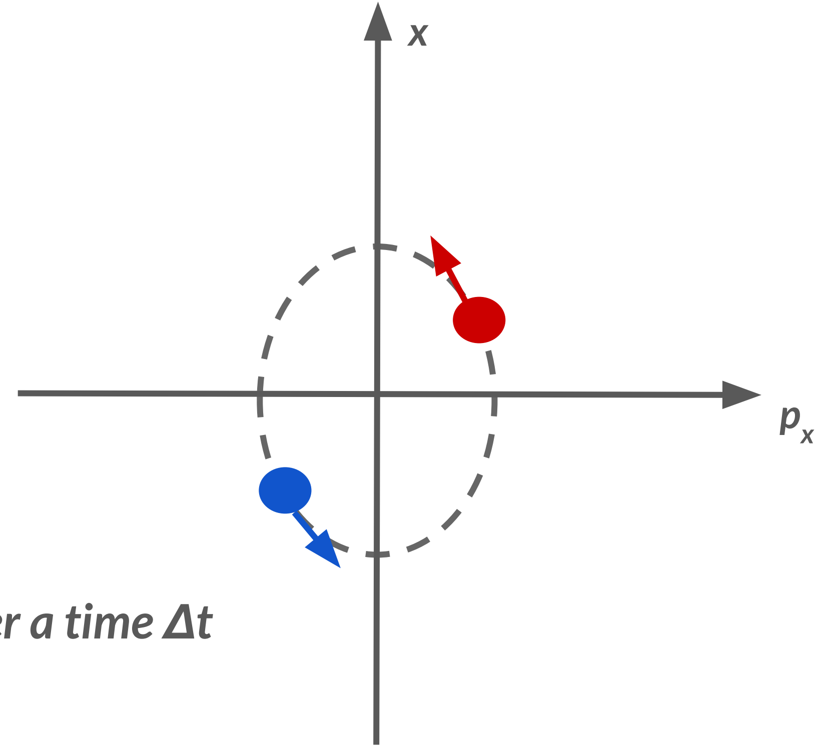

M round trips after a time Δt

A sketch of trapped-ion interferometry

Step 6: reverse trap displacement non-adiabatically

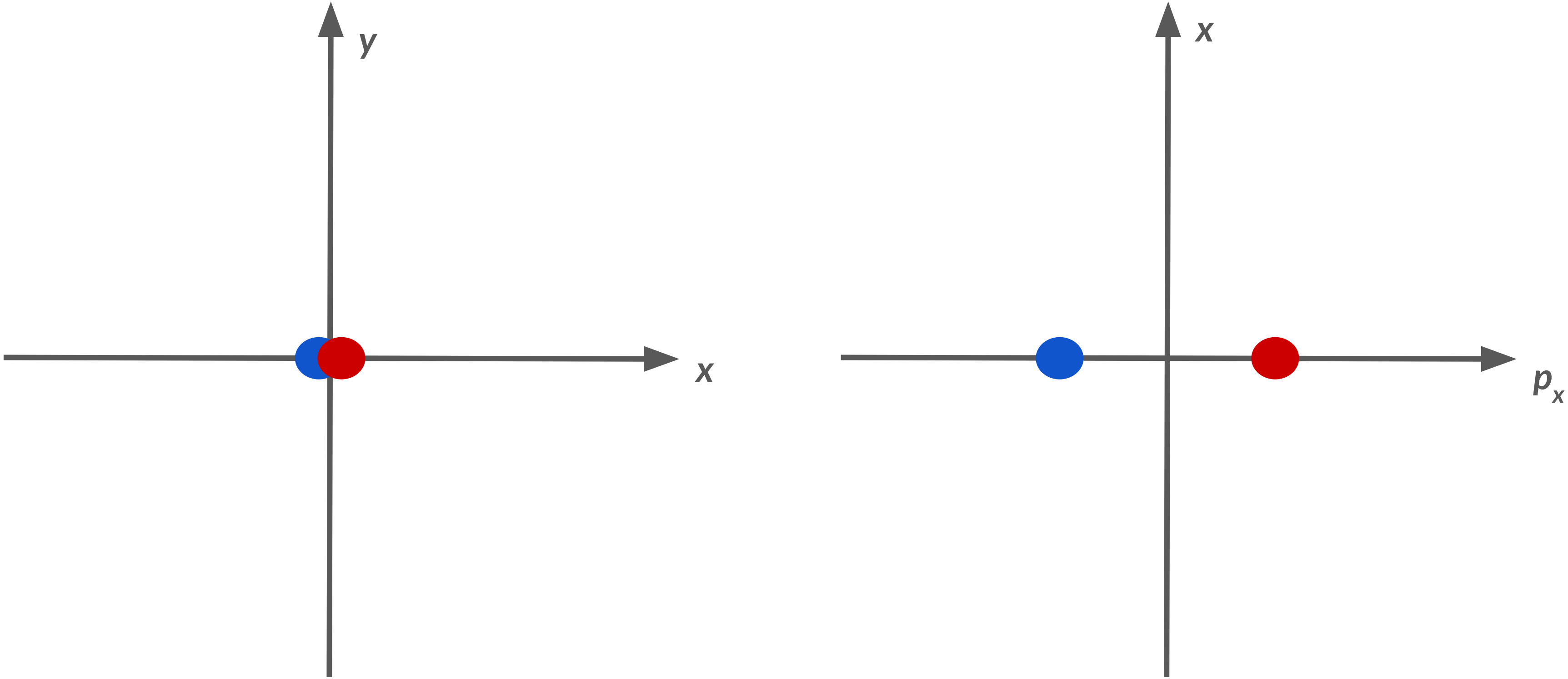

A sketch of trapped-ion interferometry

Step 7: reverse SDKs

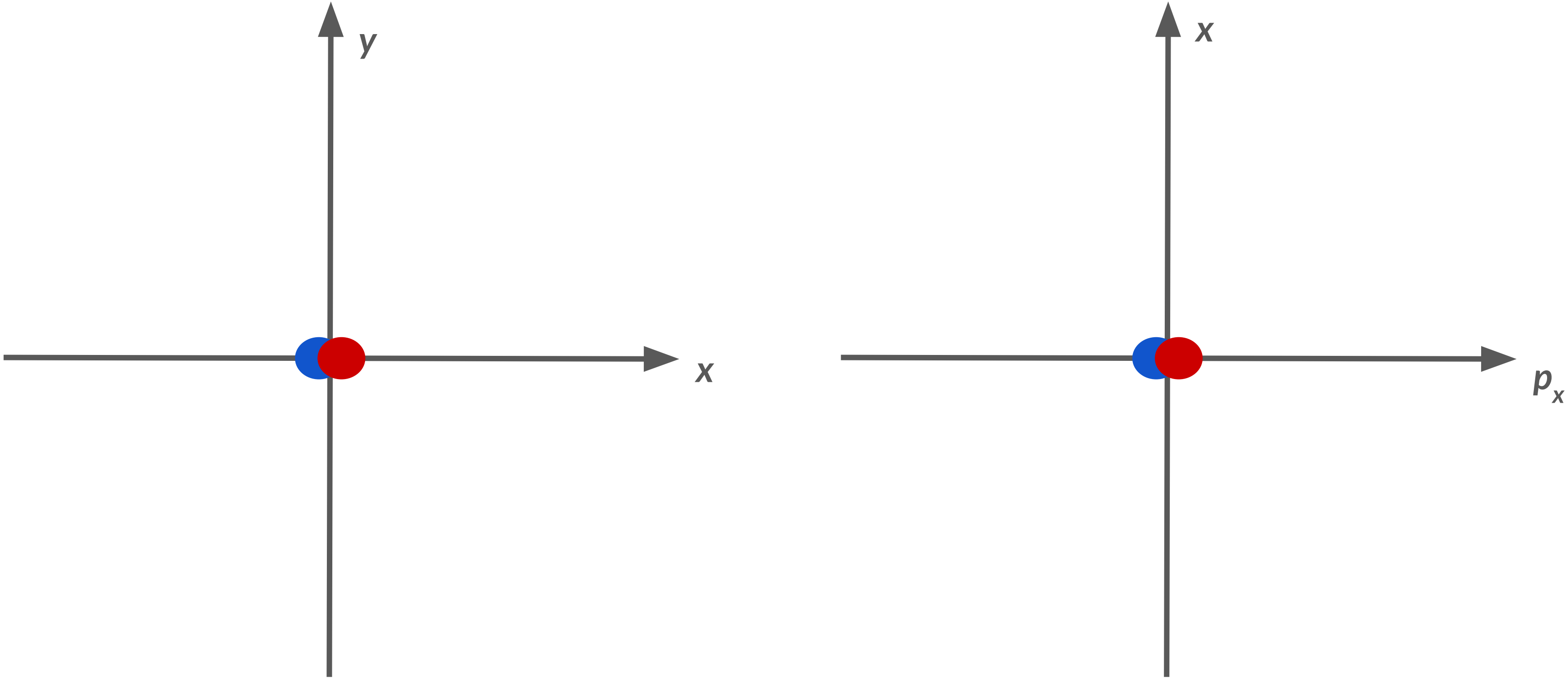

A sketch of trapped-ion interferometry

Step 8: measure the ions in the qubit spin states

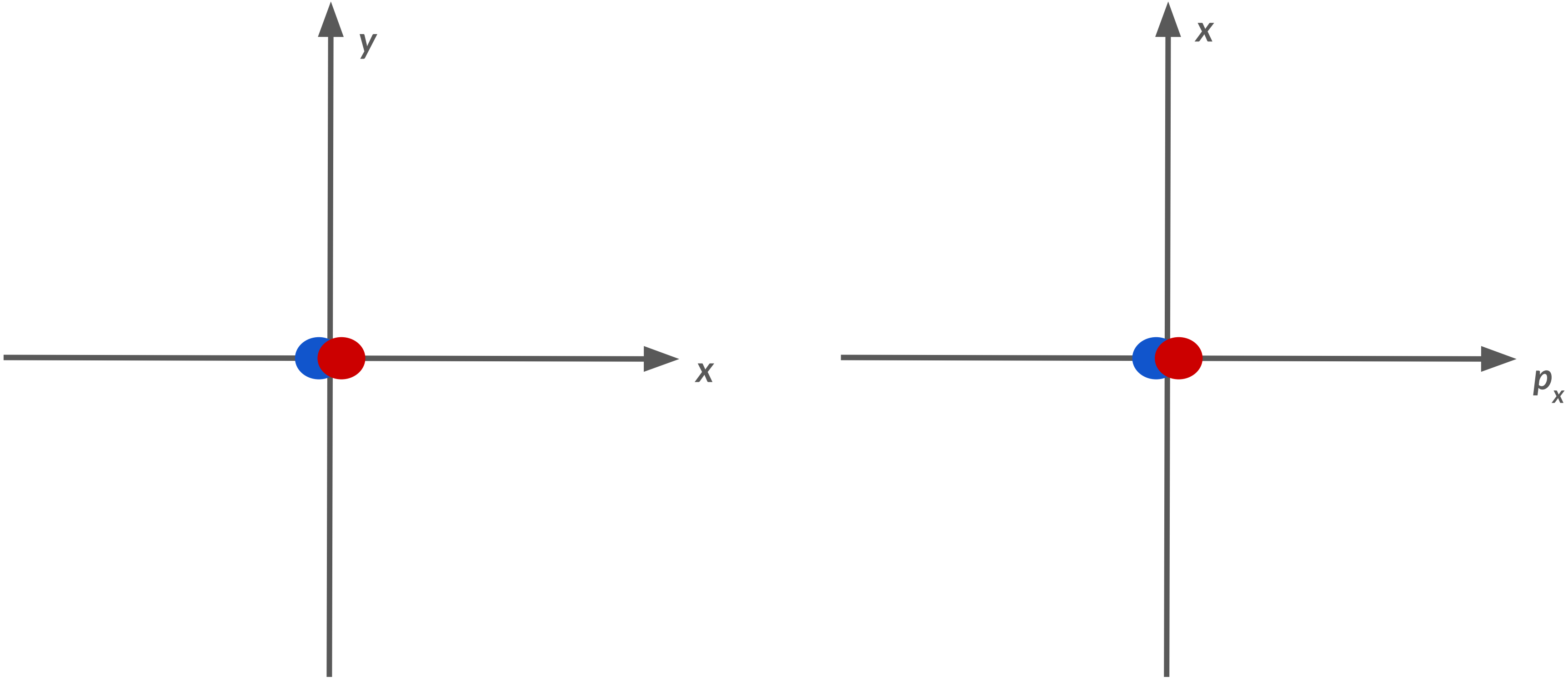

Trapped-ion interferometers as B-field sensors

Ions evolve in counterpropagating orbital motion

Trapped-ion interferometers as B-field sensors

Ions evolve in counterpropagating orbital motion

⬇

Electromagnetic phase shift only depends on the magnetic vector potential

$$\begin{aligned}\Delta\phi &= 2e\oint \mathbf{A}\cdot d\mathbf{l} \\ &\simeq 2e\int_0^{\Delta t}\mathbf{B}\cdot\frac{d\mathbf{S}}{dt}dt\end{aligned}$$

Trapped-ion interferometers as B-field sensors

Ions evolve in counterpropagating orbital motion

⬇

Electromagnetic phase shift only depends on the magnetic vector potential

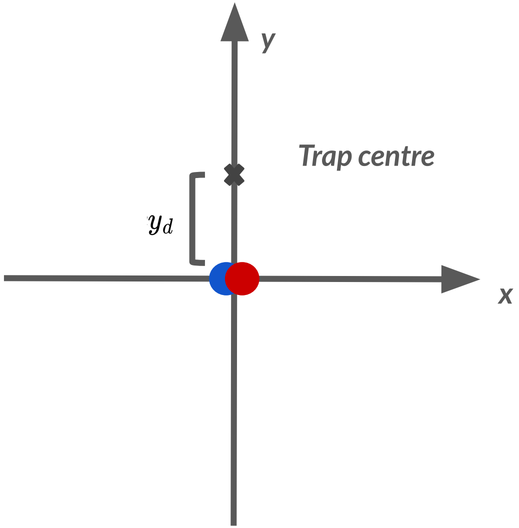

$$\Delta\phi = 2e \oint \mathbf{A} \cdot d\mathbf{l}$$

$$\simeq 2e \int_0^{\Delta t} \mathbf{B} \cdot \frac{d\mathbf{S}}{dt} dt$$

$$\frac{d\mathbf{S}}{dt} \sim y_d \frac{N\Delta k}{m_{\text{ion}}}$$

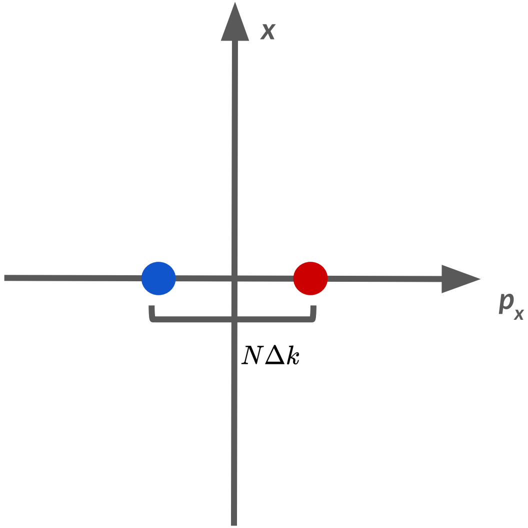

Trapped-ion interferometers as B-field sensors

Ions evolve in counterpropagating orbital motion

⬇

Electromagnetic phase shift only depends on the magnetic vector potential

$$\Delta\phi = 2e \oint \mathbf{A} \cdot d\mathbf{l}$$

$$\simeq 2e \int_0^{\Delta t} \mathbf{B} \cdot \frac{d\mathbf{S}}{dt} dt$$

$$\frac{d\mathbf{S}}{dt} \sim y_d \frac{N\Delta k}{m_{\text{ion}}}$$

Dynamical Zeeman shift with (motional) magnetic moment

$$\mu_m \sim \mu_{\text{B}} N \Delta k y_d \frac{m_e}{m_{\text{ion}}}$$

Trapped-ion interferometers as B-field sensors

$$\sqrt{S_B} = 5\times 10^{-12}\,\mathrm{T}/\sqrt{\mathrm{Hz}}\left|\mathrm{sinc}\left(\frac{\omega\Delta t}{2}\right)\right|^{-1}\left(\frac{1s}{\Delta t}\right)\left(\frac{1}{N_{\mathrm{GHZ}}}\right)$$

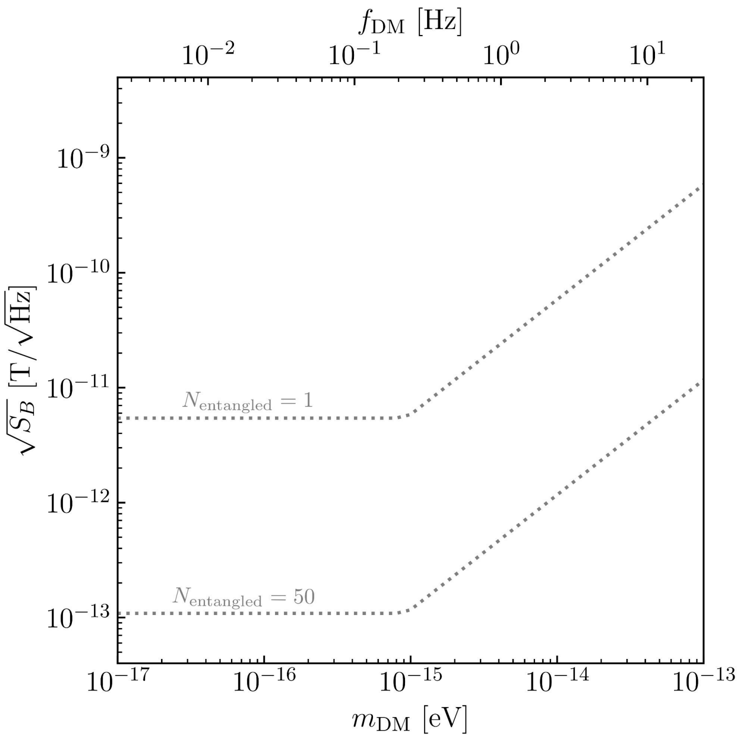

$$\mu_m \sim \mu_{\mathrm{B}} N \Delta k y_d \frac{m_e}{m_{\mathrm{ion}}}$$

[Campbell, Hamilton, JPB 2017]

$^{171}\mathrm{Yb}^+$

$$\Delta k = 4\pi/355\ \mathrm{nm}$$
$$N = 100$$
$$\Delta t = 1\ \mathrm{s}$$
$$y_d = 100\ \mu\mathrm{m}$$
$$\delta\phi = 1\ \mathrm{rad}/\sqrt{\mathrm{Hz}}$$

Trapped-ion interferometers as B-field sensors

$$\sqrt{S_B} = 5\times 10^{-12}\,\mathrm{T}/\sqrt{\mathrm{Hz}}\left|\mathrm{sinc}\left(\frac{\omega\Delta t}{2}\right)\right|^{-1}\left(\frac{1s}{\Delta t}\right)\left(\frac{1}{N_{\mathrm{GHZ}}}\right)$$

$$\mu_m \sim \mu_{\mathrm{B}} N \Delta k y_d \frac{m_e}{m_{\mathrm{ion}}}$$

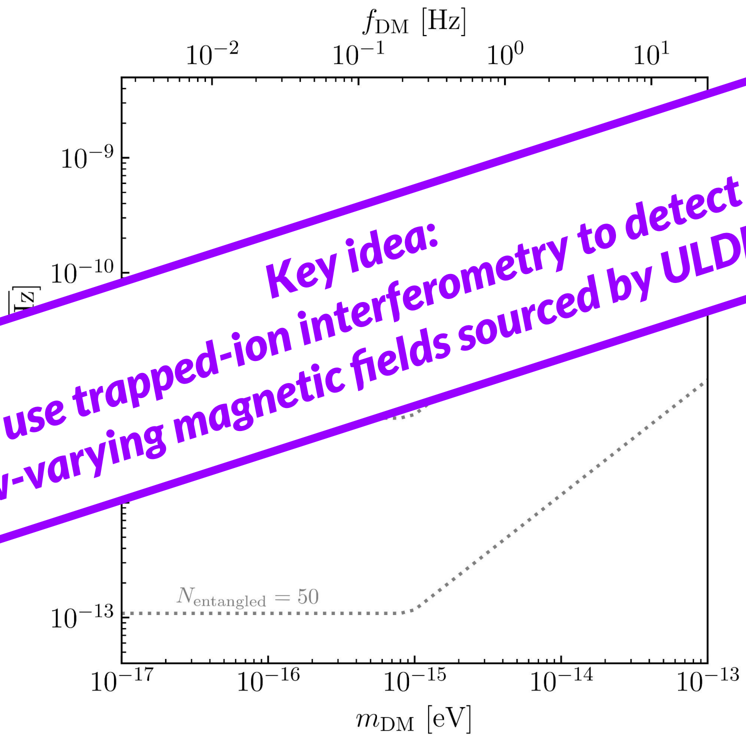

Key idea:
to use trapped-ion interferometry to detect slow-varying magnetic fields sourced by ULDM !

[Campbell, Hamilton, JPB 2017]

$^{171}\mathrm{Yb}^+$
$\Delta k = 4\pi/355$ nm
$N = 100$
$\Delta t = 1$ s
$y_d = 100\ \mu$m
$\delta\phi = 1\ \mathrm{rad}/\sqrt{\mathrm{Hz}}$

Models

Kinetically-mixed DPs

ALPs

Models

Kinetically-mixed DPs

$$\mathcal{L} \supset \epsilon m_{A'}^2 A'_\mu A^\mu$$

$$\boldsymbol{A'} \sim \frac{\sqrt{2\rho_{\rm DM}}}{\sqrt{3}m_{A'}} e^{im_{A'}t - i\boldsymbol{k}\cdot\boldsymbol{x}} \sum_i \hat{\boldsymbol{n}}_i \, e^{i\varphi_i} \ ,$$

$$\mathbf{J}_{\rm eff} = \epsilon m_{A'}^2 \mathbf{A}'$$

ALPs

Models

Kinetically-mixed DPs

$$\mathcal{L} \supset \epsilon m_{A'}^2 A'_\mu A^\mu$$

$$\boldsymbol{A'} \sim \frac{\sqrt{2\rho_{\mathrm{DM}}}}{\sqrt{3}m_{A'}} e^{im_{A'}t - i\boldsymbol{k}\cdot\boldsymbol{x}} \sum_i \hat{\boldsymbol{n}}_i \, e^{i\varphi_i} \, ,$$

$$\mathbf{J}_{\mathrm{eff}} = \epsilon m_{A'}^2 \mathbf{A}'$$

ALPs

$$\mathcal{L} \supset -\frac{g_{\mathrm{a}\gamma\gamma}}{4} a \widetilde{F}_{\mu\nu} F^{\mu\nu}$$

$$a \sim \frac{\sqrt{2\rho_{\mathrm{DM}}}}{m_a} e^{im_a t - i\boldsymbol{k}\cdot\boldsymbol{x} + i\varphi}$$

$$\mathbf{J}_{\mathrm{eff}} = -g_{a\gamma\gamma} \mathbf{B_0} \frac{\partial a}{\partial t}$$

Models

Kinetically-mixed DPs

$$\mathcal{L} \supset \epsilon m_{A'}^2 A'_\mu A^\mu$$

$$\boldsymbol{A'} \sim \frac{\sqrt{2\rho_{\rm DM}}}{\sqrt{3}m_{A'}} e^{im_{A'}t - i\boldsymbol{k}\cdot\boldsymbol{x}} \sum_i \hat{\boldsymbol{n}}_i \, e^{i\varphi_i} \, ,$$

$$\mathbf{J}_{\rm eff} = \epsilon m_{A'}^2 \mathbf{A}'$$

ALPs

$$\mathcal{L} \supset -\frac{g_{a\gamma\gamma}}{4} a\widetilde{F}_{\mu\nu}F^{\mu\nu}$$

$$a \sim \frac{\sqrt{2\rho_{\rm DM}}}{m_a} e^{im_a t - i\boldsymbol{k}\cdot\boldsymbol{x} + i\varphi}$$

$$\mathbf{J}_{\rm eff} = -g_{a\gamma\gamma}\mathbf{B_0}\frac{\partial a}{\partial t}$$

$$\nabla \times \mathbf{B} - \partial_t \mathbf{E} = \mathbf{J}_{\rm eff}$$

ULDM sources e.m. fields with angular frequency m

Models

Kinetically-mixed DPs

$$\mathcal{L} \supset \epsilon m_{A'}^2 A'_\mu A^\mu$$

$$\boldsymbol{A'} \sim \frac{\sqrt{2\rho_{\text{DM}}}}{\sqrt{3} m_{A'}} e^{i m_{A'} t - i \boldsymbol{k}\cdot\boldsymbol{x}} \sum_i \hat{\boldsymbol{n}}_i \, e^{i\varphi_i} \,,$$

$$\mathbf{J}_{\text{eff}} =$$

ALPs

$$\mathcal{L} \supset -\frac{g_{a\gamma\gamma}}{4} a \widetilde{F}_{\mu\nu} F^{\mu\nu}$$

$$\ldots_a t - i\boldsymbol{k}\cdot\boldsymbol{x} + i\varphi$$

$$\ldots_a$$

$$\mathbf{J}_{\text{eff}} = -g_{a\gamma\gamma} \mathbf{B_0} \frac{\partial a}{\partial t}$$

WARNING:
Boundary conditions -> cavity

$$\nabla \times \mathbf{B} - \partial_t \mathbf{E} = \mathbf{J}_{\text{eff}}$$

ULDM sources e.m. fields with angular frequency m

Which cavity should we use?

Since Δt > 1 s, a TI would be most sensitive to signals oscillating with frequencies below 1 Hz.

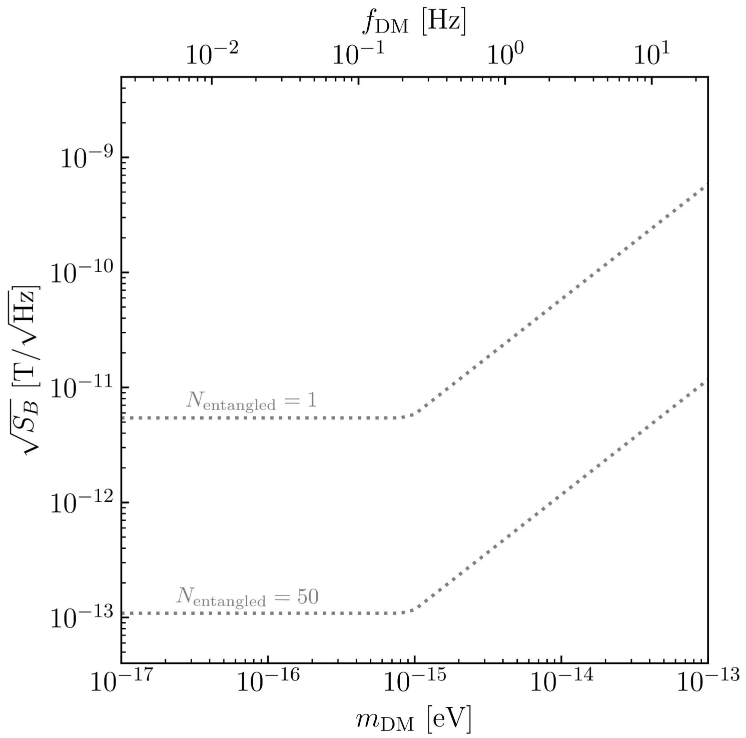

Key point:
Most sensitive to DM with mass $\lesssim 10^{-15}$ eV

Which cavity should we use?

Since Δt > 1 s, a TI would be most sensitive to signals oscillating with frequencies below 1 Hz.

We expect that shielding in the lab suppresses high-frequency magnetic fields

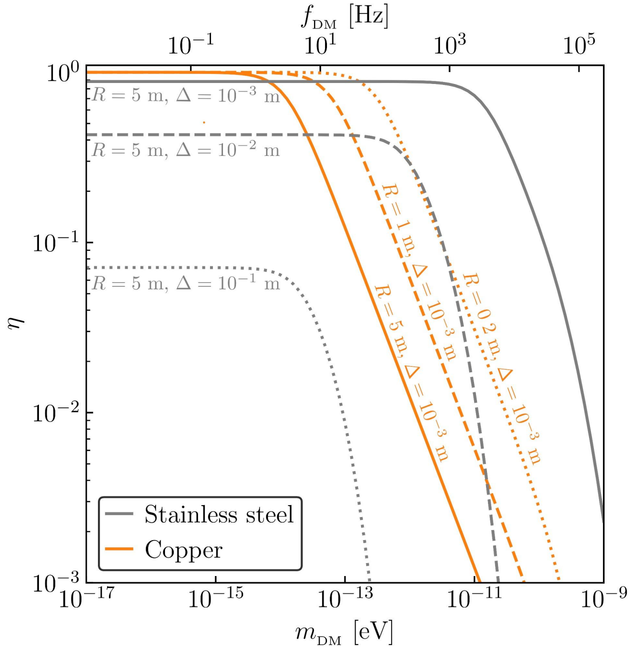

Key point:
In the lab, limited sensitivity to DM with mass $\gtrsim 10^{-13}$ eV

Which cavity should we use? The Earth-ionosphere/IPM!

Well below 10 Hz, the Earth's core and the ionosphere/interplanetary medium act as good concentric spherical conducting boundaries [Fedderke et al., PRD 2021; Arza et al., PRD 2022]

$$h \sim \mathcal{O}(100\,\mathrm{km})$$
$$R_\oplus \approx 6 \times 10^3\,\mathrm{km}$$

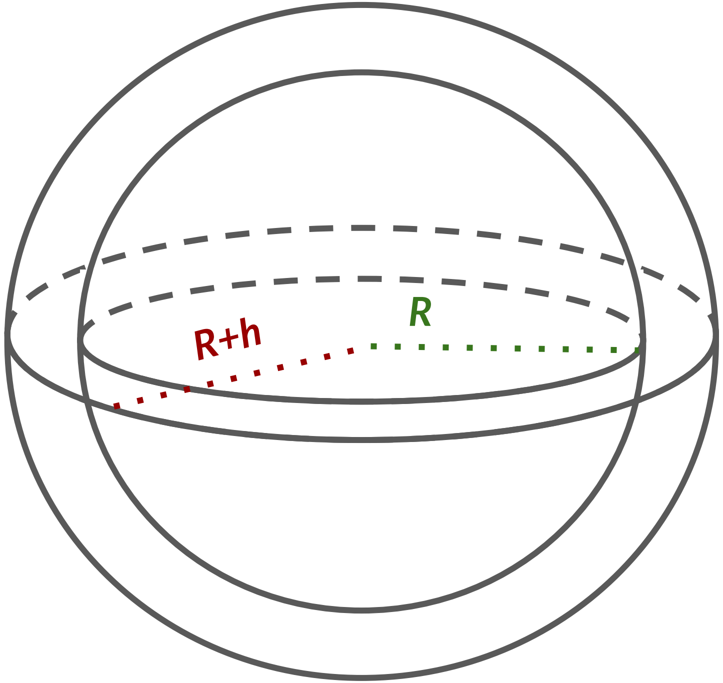

Which cavity should we use? The Earth-ionosphere/IPM!

Well below 10 Hz, the Earth's core and the ionosphere/interplanetary medium act as good concentric spherical conducting boundaries [Fedderke et al., PRD 2021; Arza et al., PRD 2022]

$$h \sim \mathcal{O}(100\,\mathrm{km})$$
$$R_\oplus \approx 6 \times 10^3\,\mathrm{km}$$

Skin depths (frequency-dependent)

Inner boundary

$$\delta\big|_{\mathrm{core}} \ll h \quad \text{for } m_{\mathrm{DM}} \gtrsim 10^{-18}\ \mathrm{eV}$$

Outer boundary

$$\delta\big|_{\mathrm{ionosphere}} \ll h \quad \text{for } 10^{-13}\ \mathrm{eV} \lesssim m_{\mathrm{DM}} \lesssim 10^{-8}\ \mathrm{eV}$$
$$\delta\big|_{\mathrm{IPM}} \ll h \quad \text{for } 10^{-22}\ \mathrm{eV} \lesssim m_{\mathrm{DM}} \lesssim 10^{-13}\ \mathrm{eV}$$

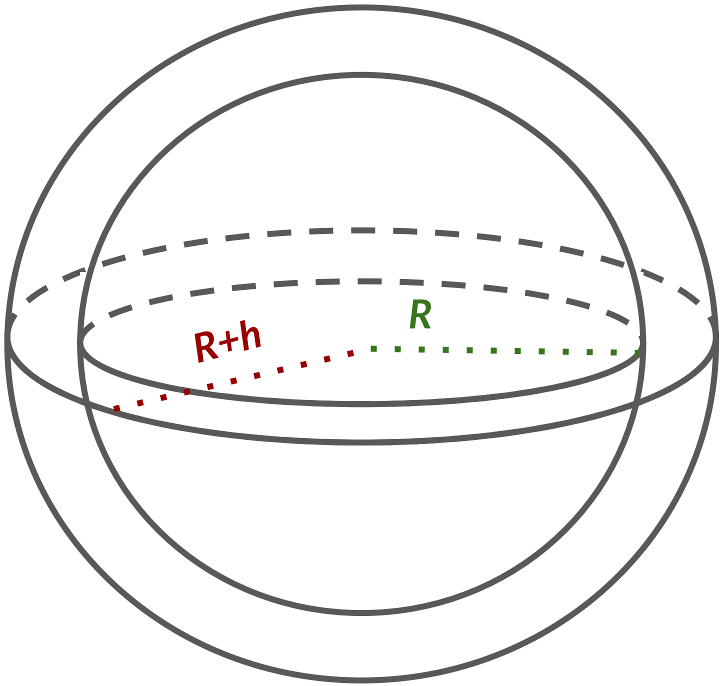

Signal in a cavity with concentric spherical boundaries

Boundary conditions

$$\hat{\mathbf{n}} \cdot \mathbf{B} = 0 \quad \hat{\mathbf{n}} \times \mathbf{E} = 0$$

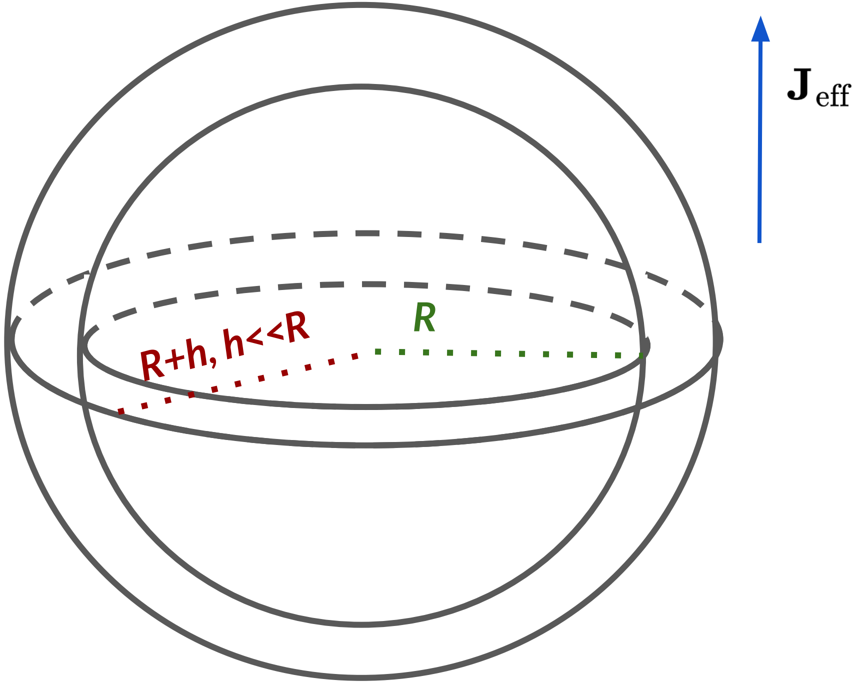

Signal in a cavity with concentric spherical boundaries

Boundary conditions

$$\hat{\mathbf{n}} \cdot \mathbf{B} = 0 \quad \hat{\mathbf{n}} \times \mathbf{E} = 0$$

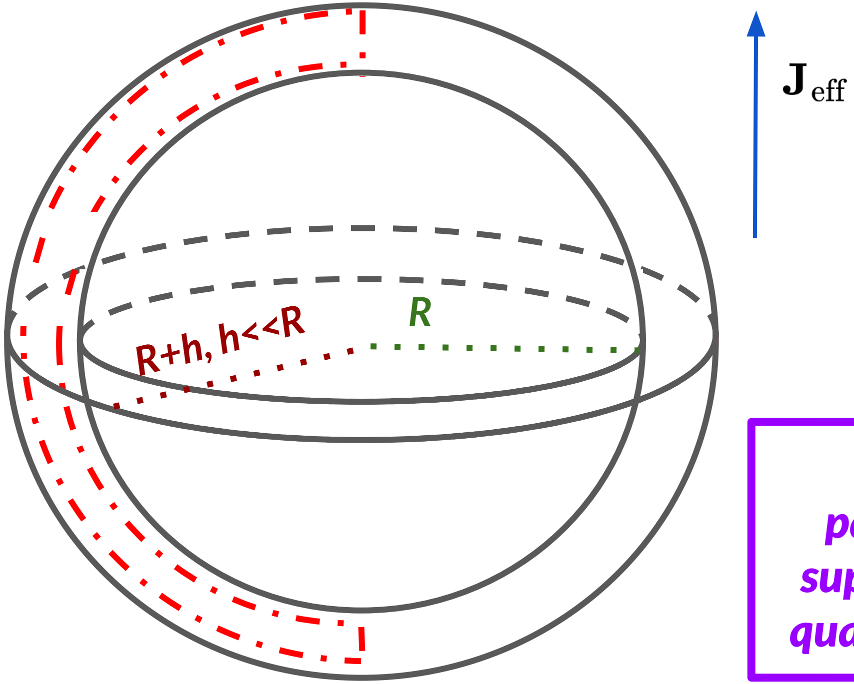

E field is parametrically suppressed in the quasistatic regime

$$\oint \mathbf{E} \cdot d\mathbf{l} = \int (\nabla \times \mathbf{E}) \cdot d\mathbf{S} = \int \partial_t \mathbf{B} \cdot d\mathbf{S} \implies E \sim (m_{\text{DM}} R)\, B$$

Signal in a cavity with concentric spherical boundaries

Boundary conditions

$$\hat{\mathbf{n}} \cdot \mathbf{B} = 0 \quad \hat{\mathbf{n}} \times \mathbf{E} = 0$$

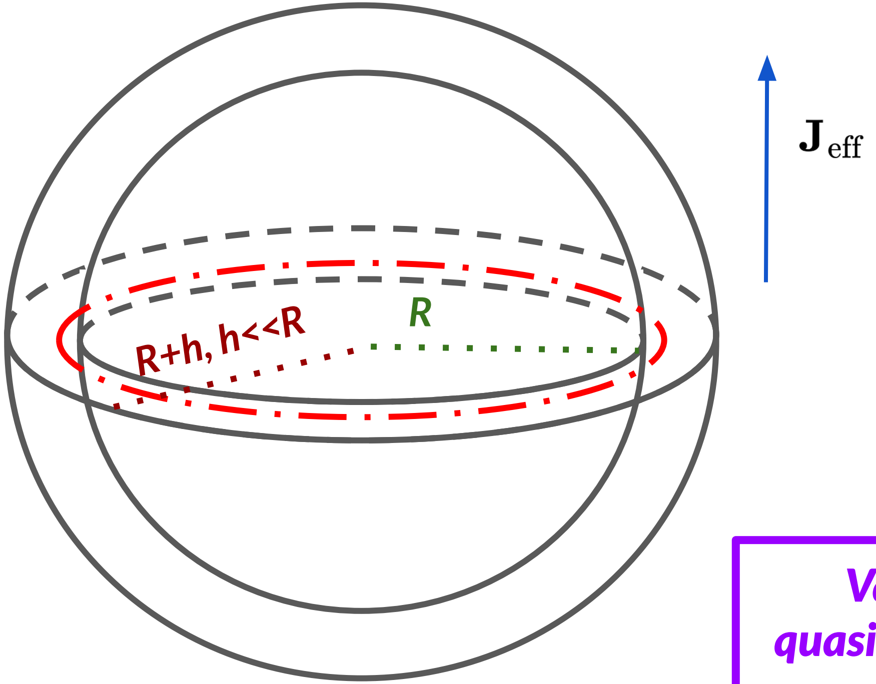

Valid in the quasistatic regime

$$\oint \mathbf{B} \cdot d\mathbf{l} = \int (\nabla \times \mathbf{B}) \cdot d\mathbf{S} = \int \mathbf{J}_{\rm eff} \cdot d\mathbf{S} \implies B \sim (m_{\rm DM} R) J_{\rm eff}$$

Signal in a cavity with concentric spherical boundaries

Boundary conditions

$$\hat{\mathbf{n}} \cdot \mathbf{B} = 0 \quad \hat{\mathbf{n}} \times \mathbf{E} = 0$$

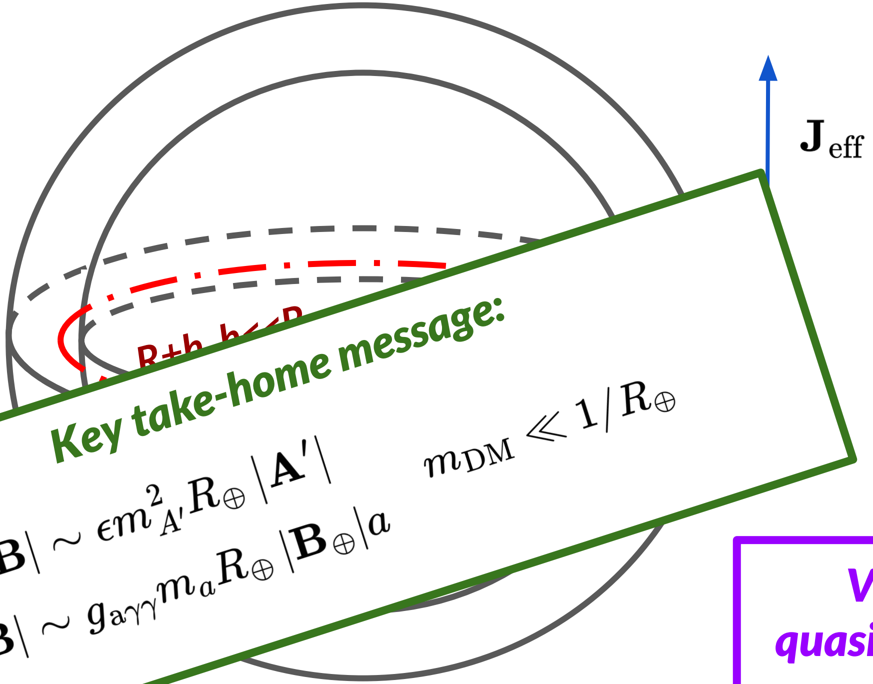

Key take-home message:

$$|\mathbf{B}| \sim \epsilon m_{A'}^2 R_\oplus |\mathbf{A}'| \qquad m_{\mathrm{DM}} \ll 1/R_\oplus$$

$$|\mathbf{B}| \sim g_{a\gamma\gamma} m_a R_\oplus |\mathbf{B}_\oplus| a$$

Valid in the quasistatic regime

$$\oint \mathbf{B} \cdot d\mathbf{l} = \int (\nabla \times \mathbf{B}) \cdot d\mathbf{S} = \int \mathbf{J}_{\mathrm{eff}} \cdot d\mathbf{S} \implies B \sim (m_{\mathrm{DM}} R) J_{\mathrm{eff}}$$

Noise projections

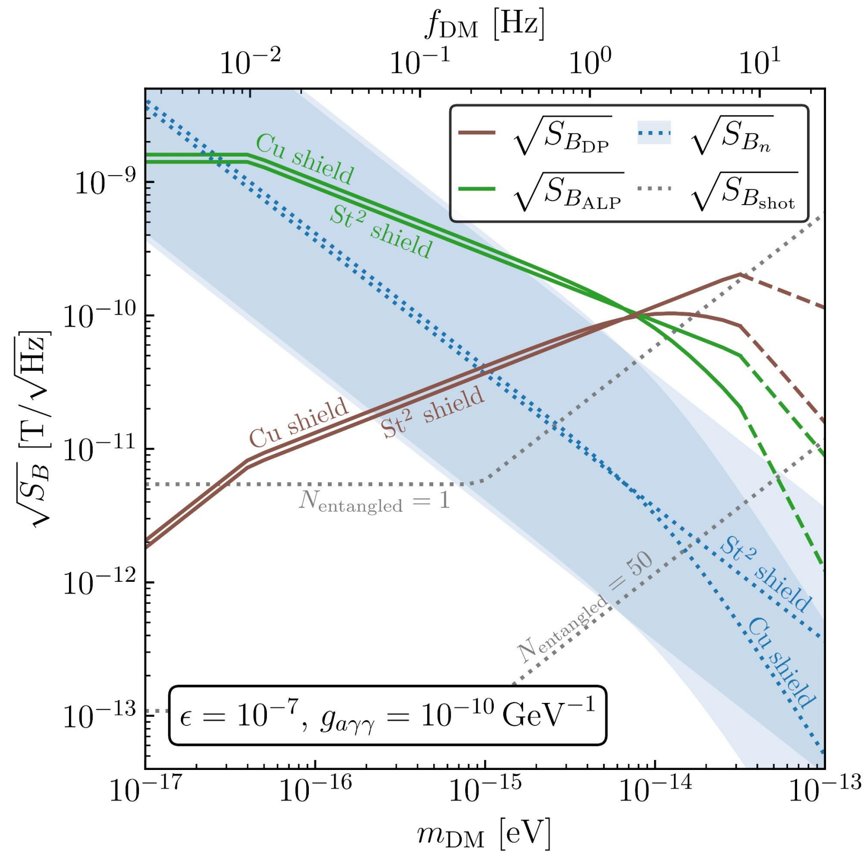

[Campbell, Hamilton, JPB 2017]

$^{171}\mathrm{Yb}^+$

$$\Delta k = 4\pi/355\ \mathrm{nm}$$
$$N = 100$$
$$\Delta t = 1\ \mathrm{s}$$
$$y_d = 100\ \mu\mathrm{m}$$
$$\delta\phi = 1\ \mathrm{rad}/\sqrt{\mathrm{Hz}}$$

Dominated by ambient magnetic noise

Fullerkrug and Fraser-Smith [2011], Constable and Constable [2023]

Projected sensitivity: DPs

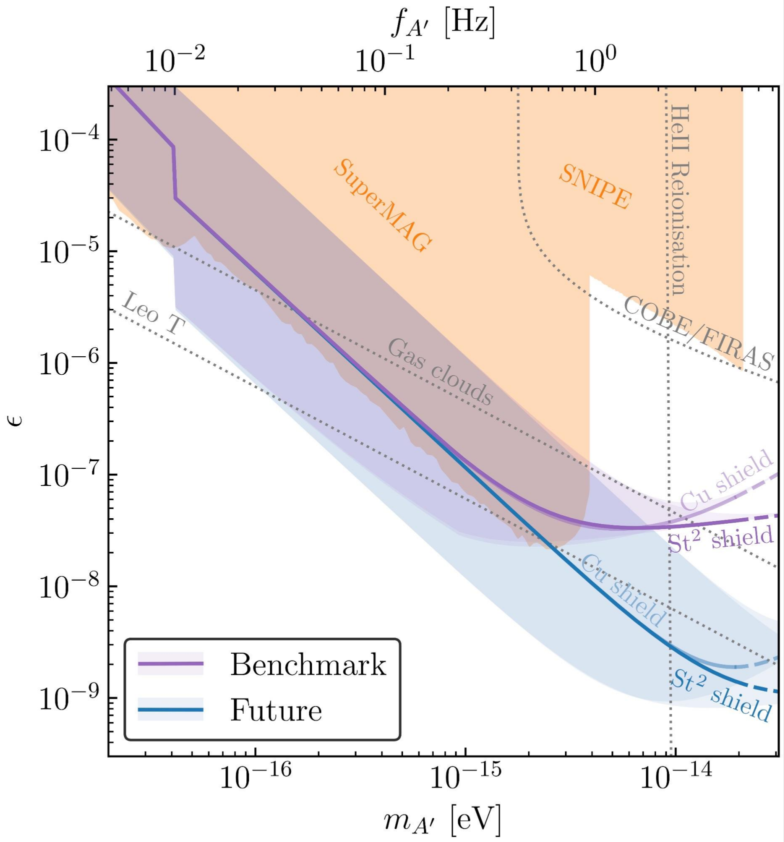

Signal is insensitive to latitude + longitude + trap orientation tangent to the Earth's surface

$$\sqrt{\left\langle \left| \widetilde{\boldsymbol{B}}_{A'}(\omega) \cdot \hat{\boldsymbol{\Sigma}} \right|^2 \right\rangle} = \epsilon m_{A'} R_{\oplus} \sqrt{\frac{\rho_{\mathrm{DM}}}{6}},$$

[Campbell, Hamilton, JPB 2017]

$^{171}\mathrm{Yb}^+$

$$\begin{aligned} \Delta k &= 4\pi/355\ \mathrm{nm} \\ N &= 100 \\ \Delta t &= 1\ \mathrm{s} \\ y_d &= 100\ \mu\mathrm{m} \\ \delta\phi &= 1\ \mathrm{rad}/\sqrt{\mathrm{Hz}} \end{aligned}$$

Projected sensitivity: ALPs

Signal is sensitive to latitude + longitude + directionality known a priori (set by the Earth's magnetic field) [IGRF 2021]

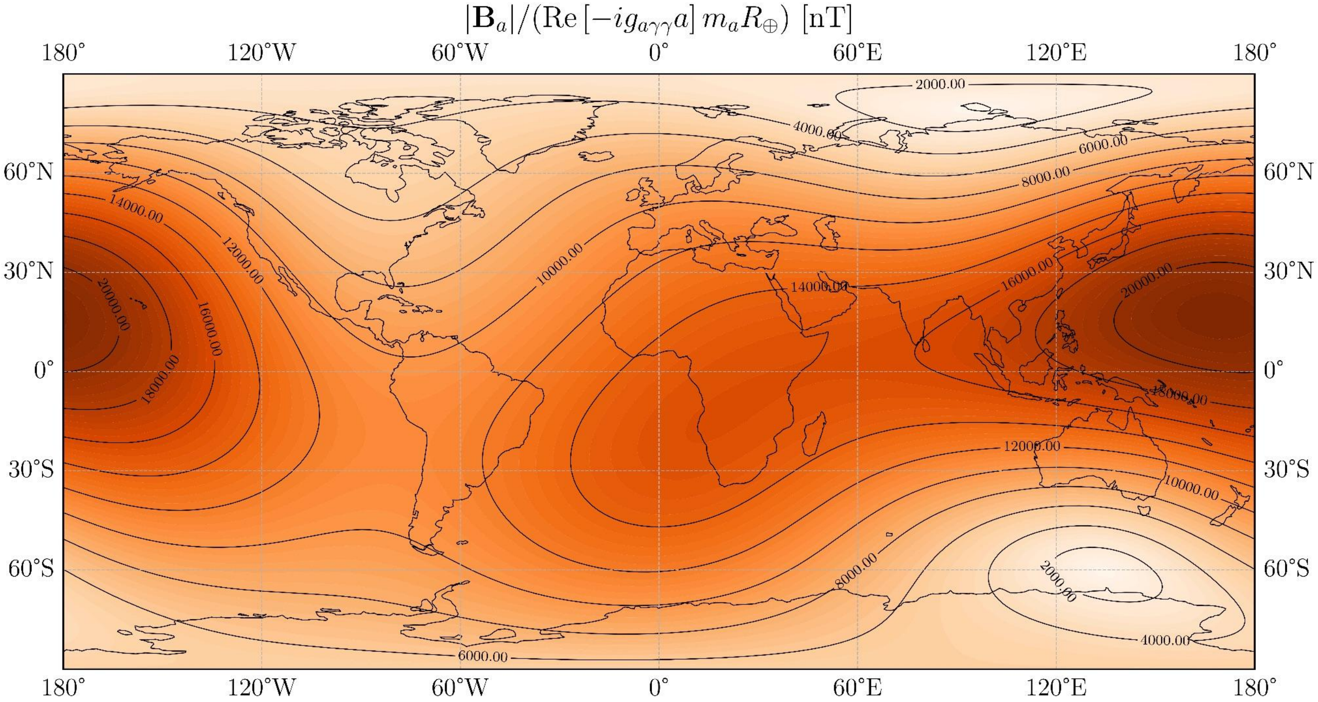

Projected sensitivity: ALPs

Signal is sensitive to latitude + longitude + directionality known a priori (set by the Earth's magnetic field)

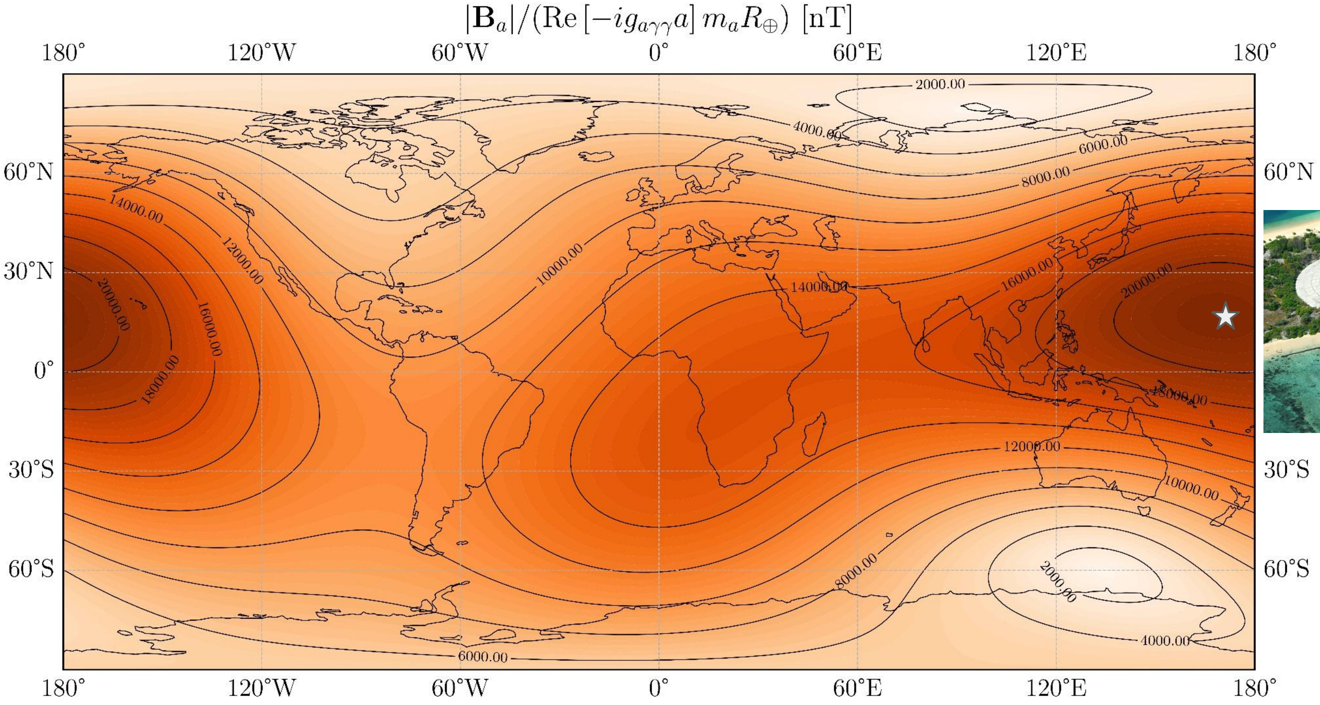

Projected sensitivity: ALPs

Signal is sensitive to latitude + longitude + directionality known a priori (set by the Earth's magnetic field)

$|\mathbf{B}_a|/(\mathrm{Re}\,[-ig_{a\gamma\gamma}a]\,m_a R_\oplus)$ [nT]

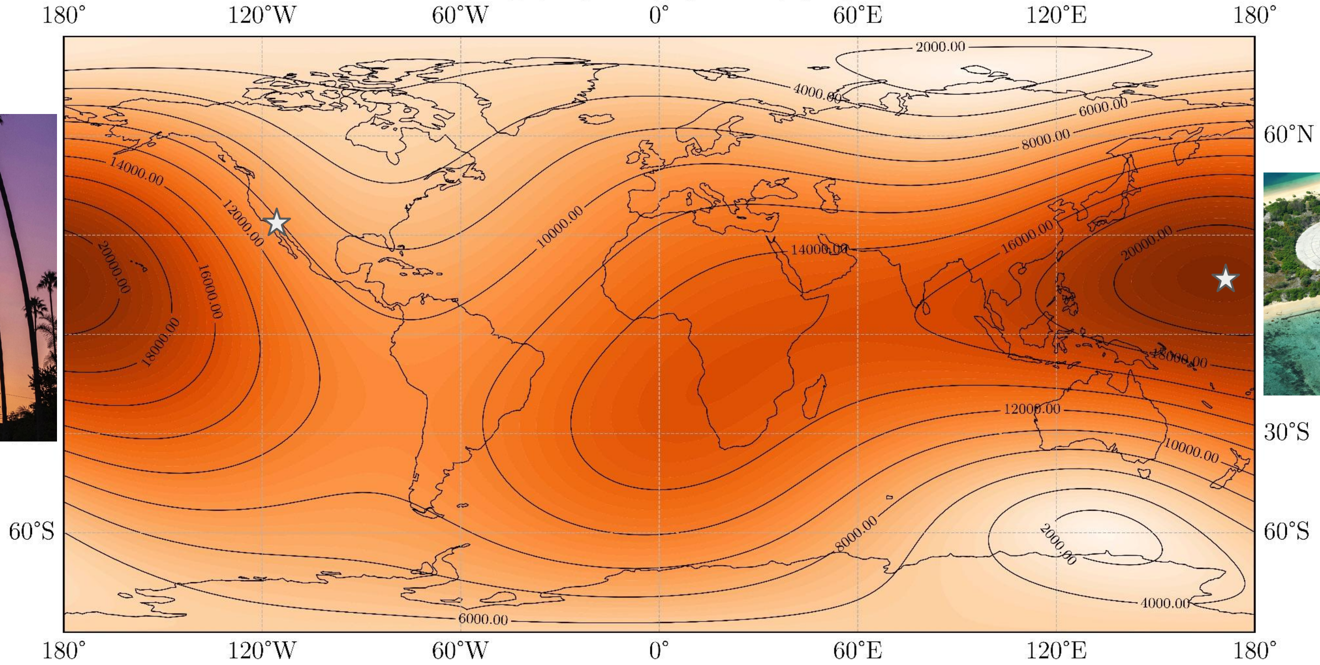

Projected sensitivity: ALPs

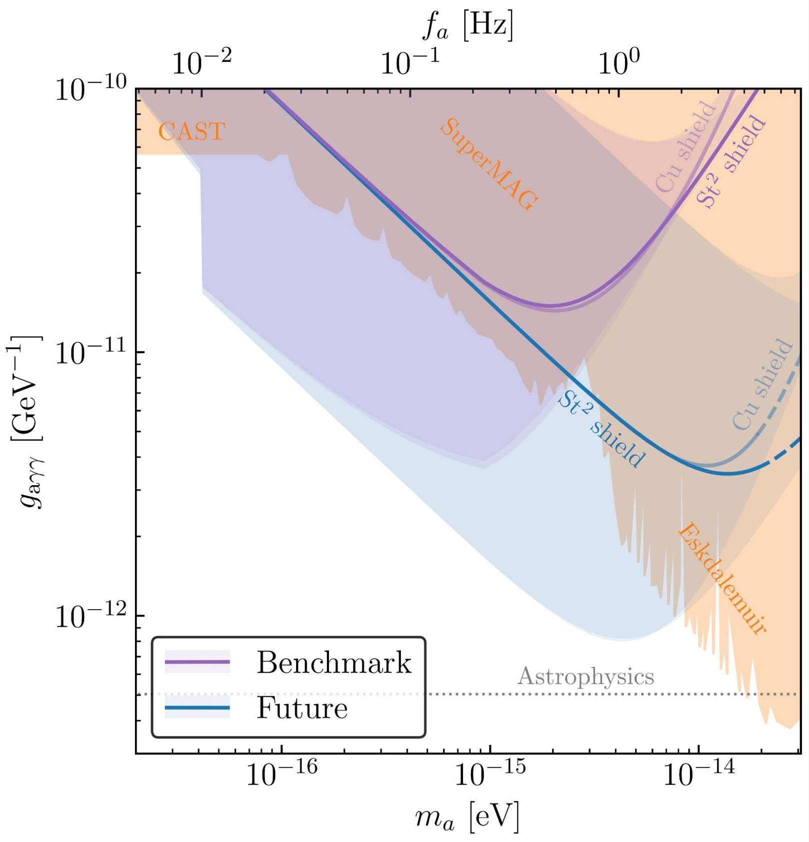

Signal is sensitive to latitude + longitude + directionality known a priori (set by the Earth's magnetic field)

$$\sqrt{\left\langle \left| \widetilde{\boldsymbol{B}}_a(\omega) \cdot \hat{\boldsymbol{\Sigma}} \right|^2 \right\rangle} = \sqrt{\left\langle \left| \widetilde{\boldsymbol{B}}_a(\omega) \right|^2 \right\rangle} \approx g_{a\gamma\gamma} R_{\oplus} \sqrt{2\rho_{\mathrm{DM}}}\,(0.11\mathrm{G})$$

[Campbell, Hamilton, JPB 2017]

$^{171}\mathrm{Yb}^{+}$

$$\begin{aligned} \Delta k &= 4\pi/355\ \mathrm{nm} \\ N &= 100 \\ \Delta t &= 1\ \mathrm{s} \\ y_d &= 100\ \mu\mathrm{m} \\ \delta\phi &= 1\ \mathrm{rad}/\sqrt{\mathrm{Hz}} \end{aligned}$$

Summary

Trapped-ion interferometers are sensitive to small B-fields via the dynamical Zeeman effect

In light of their promising projected reach, trapped-ion interferometers are poised to probe unexplored regions of ULDM parameter space!

Thank you for your attention.
Stay tuned!

BURKE INSTITUTE

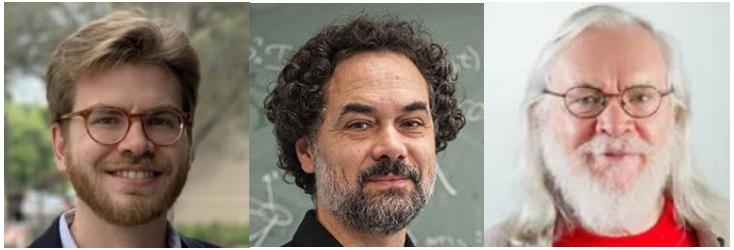

Caltech